

Cerebrospinal Fluid Proteomics Reveals Potential Pathogenic Changes in the Brains of SIV-Infected Monkeys

Gurudutt Pendyala,^{†,‡} Sunia A. Trauger,[§] Ewa Kalisiak,[§] Ronald J. Ellis,^{||} Gary Siuzdak,[§] and Howard S. Fox^{*,†,‡}

Department of Pharmacology and Experimental Neuroscience, University of Nebraska Medical Center, Omaha, Nebraska 68198, Molecular and Integrative Neurosciences Department, The Scripps Research Institute, 10550 North Torrey Pines Road, La Jolla, California 92037, Department of Molecular Biology and Center for Mass Spectrometry, The Scripps Research Institute, 10550 North Torrey Pines Road, La Jolla, California 92037, and Department of Neurosciences and HIV Neurobehavioral Research Center, University of California, 150 West Washington St, San Diego, California 92103

Received October 11, 2008

The HIV-1-associated neurocognitive disorder occurs in approximately one-third of infected individuals. It has persisted in the current era of antiretroviral therapy, and its study is complicated by the lack of biomarkers for this condition. Since the cerebrospinal fluid is the most proximal biofluid to the site of pathology, we studied the cerebrospinal fluid in a nonhuman primate model for HIV-1-associated neurocognitive disorder. Here we present a simple and efficient liquid chromatography-coupled mass spectrometry-based proteomics approach that utilizes small amounts of cerebrospinal fluid. First, we demonstrate the validity of the methodology using human cerebrospinal fluid. Next, using the simian immunodeficiency virus-infected monkey model, we show its efficacy in identifying proteins such as alpha-1-antitrypsin, complement C3, hemopexin, IgM heavy chain, and plasminogen, whose increased expression is linked to disease. Finally, we find that the increase in cerebrospinal fluid proteins is linked to increased expression of their genes in the brain parenchyma, revealing that the cerebrospinal fluid alterations identified reflect changes in the brain itself and not merely leakage of the blood-brain or blood-cerebrospinal fluid barriers. This study reveals new central nervous system alterations in lentivirus-induced neurological disease, and this technique can be applied to other systems in which limited amounts of biofluids can be obtained.

Keywords: SIV • HIV • proteomics • CSF • dementia • biomarker • neuropathology • monkey

Introduction

HIV-associated neurological disorders (HAND) have persisted in the current era of highly active antiretroviral therapy (HAART).¹ While the incidence of severe dementia has decreased, the prevalence of both motor and cognitive neurological disorders may actually be increasing.² Similarly to many neurodegenerative disorders, biomarkers to predict those at risk for HAND, its progression, and response to therapy are lacking.

A biomarker has been defined as any characteristic that is objectively measured and evaluated as an indicator of normal biological, pathogenic processes or pharmacological responses to a therapeutic intervention.³ Discovery of disease specific biomarkers has been an important challenge in biomedical research as well as clinical medicine. While biomarkers can

have great utility in diagnostic, prognostic, and therapeutic determinations, the unique cellular and phenotypic complexity of the brain has hindered biomarker identification in neurological disorders. Though extensive effort has been devoted to the search for reliable biomarkers across a spectrum of neurodegenerative diseases, the success rate has been fairly disappointing, especially for the most easily accessible biofluid, plasma.⁴

Among the body fluids, the cerebrospinal fluid (CSF), which occupies the ventricular and subarachnoid spaces in the brain,^{5,6} provides an ideal window for insights into mechanisms of neurodegeneration. Since it interacts directly with the extracellular milieu of the brain, the CSF is a unique matrix for the detection of biochemical changes associated with neurodegeneration and the progression of disease in the central nervous system (CNS). The protein component of CSF consists of brain-derived proteins as well as many proteins that are also abundant in plasma.⁷ The complexity and great dynamic range of protein concentrations and protein heterogeneity in the CSF create significant challenges to the existing proteomic technologies.⁸ To address these challenges, several advances have been made on two fronts: enrichment of potential proteins of

* To whom correspondence should be addressed. University of Nebraska Medical Center, 985800 Nebraska Medical Center, Omaha, NE 68198-5800. E-mail: hfox@unmc.edu.

[†] University of Nebraska Medical Center.

[‡] Molecular and Integrative Neurosciences Department, The Scripps Research Institute.

[§] Department of Molecular Biology and Center for Mass Spectrometry, The Scripps Research Institute.

^{||} University of California.

interest expressed at lower levels via immunodepletion of abundant proteins⁹ and an improved ability to separate the great number of peptides resulting from protein digestion through multidimensional chromatography prior to mass spectrometry (MS).¹⁰ However these can not only require a relatively large amount of starting material, which can be difficult for CSF, but the greater number of manipulations can itself add variability to the results of proteomic experiments, compounding the pre-existing biologic variability in the subjects under study.

To help address these issues, we asked whether a more streamlined proteomic approach could be used to identify protein biomarkers in the CSF, utilizing the simian immunodeficiency virus (SIV)/rhesus monkey model of HAND.^{11,12} Here we present a simplified, efficient method for the proteomic analysis of small amounts of human or experimental animal CSF, show its efficacy in identifying differentially expressed proteins in SIV-infected monkeys, and determine whether the genes encoding these proteins are up-regulated in the infected brains.

Experimental Procedures

Experimental Subjects. Human volunteers were recruited under IRB approval from the University of California at San Diego, following NIH guidelines; written informed consent was obtained. The volunteers were healthy and ambulatory, with no subclinical disease as revealed by routine clinical diagnostic tests. Rhesus monkeys (*Macaca mulatta*), free of type D simian retroviruses, Cercopithecine Herpesvirus 1, simian T-cell leukemia virus type 1, and SIV, were acquired from Charles River (Key Lois, Florida) and Covance (Alice, Texas) and used for the experiments under IACUC approval from The Scripps Research Institute, following NIH/USDA guidelines.

CSF Analysis. For humans, CSF was obtained by lumbar puncture. Human CSF was processed within 1 h by centrifugation at 300g to remove cells, and the supernatant then aliquoted and stored at -80°C until further use. For the four monkeys used for proteomics, CSF was obtained by suboccipital puncture of the cisterna magna from animals under ketamine anesthesia both prior to infection and then immediately prior to necropsy. Monkey CSF was collected, immediately placed on ice, centrifuged at 1000g within 1 h to remove cells, then aliquoted and stored at -80°C until further use.

For protein isolation, 250 μL of human CSF from each of five individuals was pooled, whereas for the monkey studies separate 100 μL aliquots of CSF from each monkey before infection and at necropsy were used, and extracted with 4 volumes of ice-cold methanol. The samples were vortexed and incubated at -20°C for 1 h. The samples were centrifuged at 14 000g for 20 min at 4°C , the supernatant removed for other studies, and the protein pellets were dissolved in RapiGEST (Waters Inc., Milford, MA). The protein concentration was measured using the Bradford method (BioRad, Hercules, CA) using bovine serum albumin as a standard.

Two-hundred micrograms of protein from the pooled human sample, and 10 μg of protein from each monkey sample, was reduced with 10 mM D,L-dithiothreitol (Sigma-Aldrich, St. Louis, MO) at 65°C for 1 h followed by alkylation with 55 mM iodoacetamide (Sigma-Aldrich) at room temperature for 30 min in the dark. The samples were then digested with trypsin (Promega, Madison, WI) at the ratio 1:30 (w/w) at 37°C overnight. The next day, trypsin action was stopped (and RapiGEST precipitated) by the addition of concentrated hy-

drochloric acid (Fisher Scientific, Pittsburgh, PA) and the RapiGEST was removed by centrifugation at 14 000g for 20 min at 4°C . The supernatants were carefully removed, concentrated in a SpeedVac, and reconstituted in 0.1% formic acid (Fisher Scientific, Pittsburgh, PA) before loading onto the column.

One-Dimensional Liquid Chromatography (LC) and Mass Spectrometry. A fused silica capillary (75 μm internal diameter (ID), 360 μm outer diameter, 14 cm length) was pulled to a narrow tip with the ID smaller than 5 μm using a Sutter P-2000 laser puller (Sutter Instrument Company, Novato, CA) and packed with 5 μm Zorbax SB-C18 packing material (Agilent Technologies, Santa Clara, CA). This served both as the analytical column and a nanoelectrospray tip. The peptide mixtures were loaded onto this column using an in-house constructed pressure cell and the samples were directly sprayed into the LTQ mass spectrometer (Thermo Scientific, Waltham, MA) using an Agilent 1100 LC/MSD Trap system coupled directly to an Agilent 1100 nanopump and a microautosampler. The gradient consisted of 5% acetonitrile (ACN) (Fisher Scientific) for 30 min followed by a gradient to 35% ACN for 85 min, 55% ACN for 10 min, 70% ACN for 15 min, and re-equilibrated with 5% ACN for 15 min. A wash step was included after each sample analysis to prevent any carryover. A MS scan range of 400–2000 m/z was employed in the positive mode, followed by data-dependent MS/MS on 5 most abundant ions in each MS spectrum. Redundancy was reduced using dynamic exclusion.

Proteomic Data Analysis. Mammalian proteins from the NCBI database (20051012) were searched using Spectrum Mill search engine (Rev A.03.03.072, Agilent). Tolerances of 2.5 Da for precursor ions and 0.7 Da for fragment ions were used with a trypsin restriction and a maximum number of missed cleavages specified as 2. Carbamidomethyl was considered as a fixed modification, and an oxidation of methionine was permitted as a variable modification. The criteria used for peptide validation were the following: a threshold score of 11.0 for 2+ ions, a % scored peak intensity (SPI) of 60. For 3+ ions, a score threshold of 13 and a % SPI threshold of 70 were used. For both charge states, the score threshold used for the forward-reverse scores 2, and for the rank 1-rank 2 score was also set to 2.0. For 3+ ions, a score threshold of 12.0, a % SPI of 70, a forward-reverse score threshold of 2, and a rank of 1–2 score threshold of 2.0 was used. Since protein identifications with 2 and more unique peptides were used, the false discovery is expected to be negligible.

Spectrum counting was used for relative protein quantitation.^{13–15} The number of valid MS/MS spectra for each protein was normalized by dividing that value by the total number of MS/MS spectra in each sample and multiplying by 100, yielding its relative abundance. Calculations were performed with Excel (Microsoft Corp., Redmond, WA). Correlation analysis between the mean and standard deviation was performed using Prism (GraphPad Software, San Diego, CA). To examine differential protein abundance or gene expression, a paired or unpaired (respectively) student's *t* test (Excel) was used for statistical analysis.

Monkey Necropsy, RNA Isolation, and Histopathology. For the four animals used above, and the eight others used for RNA studies, animals were sacrificed due to predetermined criteria of development of symptomatic simian AIDS. For the nine uninfected control animals, sacrifice was timed by experimental protocol. For necropsy, animals were lethally anesthetized, extensively perfused with PBS containing 1 U/mL heparin to

Table 1. Sequence of Primers and Probes Used for Quantitative Real-Time PCR for the Indicated Rhesus Genes^a

gene	oligo sequence
IgM heavy chain	For: CCACCTACGACAGTGTGACC Rev: CTCTCGGAGATGTTGGTGTG Pro: ACCTGGACCCGCCAGAATGG
Hemopexin	For: TTGCTGAAGGTGAGACCAAG Rev: TGGTAGCATCAAAGTCCAG Pro: CCCAGACGTGACTGAACGCTGC
Complement 3	For: TCCTGGACTGCTGCAACTAC Rev: TCTCTTCTGCGATGATGTCC Pro: TACTCCTGGCCAGGCCAGG
Plasminogen	For: CCAACTTCCAGATGCAGAGA Rev: GCATGGTGTCCAGTAACAG Pro: ACCGAGCAAGAAGGCAACCA
Alpha-1-antitrypsin	For: TCCCACCTCTACCTGTCTC Rev: AGCATGACTGAGGCAGACAC Pro: CATGCCGGCCTGACGCTT
18S	For: CGGCTACCACATCCAAGGAA Rev: GCTGGAATTACCGCGGCT Pro: TGCTGGCACCAGACTTGCCCTC
GAPDH	For: GCACCACCAACTGCTTAGCAC Rev: TCTTCTGGGTGGCAGTGTAT Pro: TCGTGAAGGACTCATGACCACAGTCC
TBP	For: AAAGACCATTGCACTTCGTG Rev: GGTTCTGTGGCTCTCTTATCC Pro: TCCCAAGCGGTTTGCTGCAG

^aForward and reverse primers are indicated by For and Rev, respectively. Probes are indicated by Pro, and were labeled with FAM as the fluorochrome and TAMRA as the quencher.

clear blood-borne cells from the brain, and vital organs removed for pathological and other studies. The hippocampus was dissected from the brains, snap frozen, and RNA isolated using Trizol (Invitrogen, Carlsbad, CA) and quantified spectrophotometrically. For neuropathological analysis tissue blocks from standardized regions of the brain were taken, fixed in formalin, embedded in paraffin, cut in 5 μ m thick sections, stained, and examined microscopically.

Quantitative Real Time PCR. Two micrograms of RNA from the hippocampus of control and infected monkeys was used for reverse transcription. In a 50 μ L reaction, reverse transcription (RT) was carried out using the Superscript kit (Invitrogen) for 1 h at 42 °C, followed by 70 °C for 5 min to inactivate the RT reagents. RNase H (New England Biolabs, Beverly, MA) treatment was then performed at 37 °C for 20 min. An equal volume of RNase and DNase free water was then added to the reactions.

Real time PCR was performed using gene-specific primers and probes (Table 1). The primers and probe sequences were designed for rhesus sequences using the Genescript online tool (<https://www.genescript.com/ssi-bin/app/primer>) and obtained from Eurogentec (San Diego, CA). To carry out quantitative real time PCR, 2 μ L of the (1:10 diluted) cDNA was used for assaying the amount of 18S endogenous rRNA; 5 μ L (undiluted) each for all other genes. All reactions were performed in duplicate. 12.5 μ L of platinum qPCR UDG Supermix (Invitrogen) was added per 25 μ L reaction. The reaction mixture was brought to a final concentration of 5 mM MgCl₂. Real time PCR was performed in 96-well plate on a Stratagene MX3000p machine (Stratagene, La Jolla, CA). The delta Ct (dCt) method was performed to determine relative concentrations, using the average of the Ct of 18S, GAPDH and TBP as the normalizing value. Relative units (2^{dCt}) were calculated and used here as a

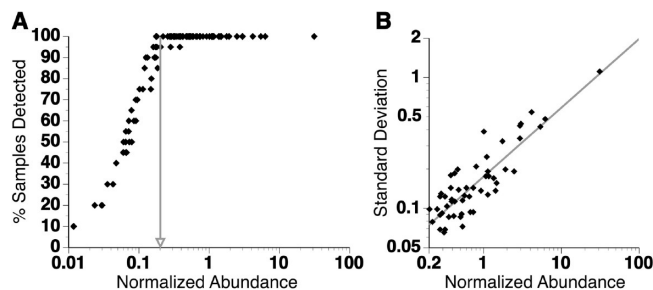


Figure 1. Precision analysis. (A) Detection of a given protein in the 20 replicate samples. The percentage of the samples in which the protein was detected is indicated on the Y-axis, and the normalized abundance on the X-axis. The gray arrow indicates an abundance of 0.2. (B) Standard deviation of the proteins with a normalized abundance of >0.2 is indicated on the Y-axis, and the normalized abundance on the X-axis, plotted on a log scale to allow visualization of the range of data. A power function was used to plot the line shown in gray [standard deviation = (0.175)(normalized abundance)^{-0.527}], $r^2 = 0.758$.

measure of mRNA expression. Unpaired student's *t* tests (Excel) were used for statistical analysis.

Immunohistochemistry. Immunohistochemical staining followed a basic indirect protocol on formalin-fixed, paraffin-embedded sections, using heating in a Tris-Urea (pH 9.5) solution as the antigen retrieval method. Sections were incubated with mouse monoclonal antihuman IgM (1 μ g/mL, CM7; Santa Cruz Biotechnologies, Santa Cruz, CA) or rabbit polyclonal antihuman plasminogen (10 μ g/mL, H-90, Santa Cruz Biotechnologies) overnight, detected with the PicturePlus universal secondary antibody-horseradish peroxidase polymer reagent (Zymed, San Francisco, CA) and developed with the NovaRed chromogen (Vector Laboratories, Burlingame, CA), followed by a hematoxylin counterstain (Sigma-Aldrich). Controls included omission of the primary antibody and use of irrelevant primary antibodies. Image capture was performed with a Spot RT Color CCD camera with Spot RT software (Spot Diagnostic Instruments, Sterling Heights, MI) using a Leica Diaplan microscope (Leica, Deerfield, IL). Figures were assembled with Adobe Photoshop (Adobe Systems, San Jose, CA).

Results

We initially examined whether shotgun proteomic analysis of relatively small amounts of CSF would yield data suitable for analysis. We first determined the technical variability of the LC-MS/MS analysis by examining twenty aliquots of protein obtained from a pooled sample of human CSF. Since normal human lumbar CSF has 150–450 μ g protein/mL, we used an amount that could be routinely obtained from relatively small volumes of CSF, 10 μ g of protein, in each run. In these twenty replicate samples, total of 93 proteins were detected that were identified by at least 2 unique peptides. Fifty-three proteins were found with a normalized abundance of >0.2. Fifty of these were found in all 20 samples, whereas the other three were found in 19 of the 20. For those with a normalized abundance of <0.2, their reproducibility of detection in the replicate samples dropped quickly as abundance decreased (Figure 1A).

We next examined the variability of the measurements for these 53 proteins with a normalized abundance of >0.2. Examination of the standard deviation of the normalized replicate measurements versus the mean of the normalized replicate measurements revealed a strong positive relationship

Table 2. Proteins up and down Regulated by SIVE along with the Fold Change^a

protein identified	distinct peptides	fold change	p value
IgM heavy chain	8	+Inf.	0.010
Hemopexin	4	+3.16	0.003
Alpha-1-antitrypsin	6	+2.91	0.008
Plasminogen	12	+2.49	0.006
Complement C3	23	+1.91	0.001
Ectonucleotide Pyrophosphatase 2	14	-3.34	0.007
Fibronectin 1	17	-3.60	0.007
Prostaglandin D2 Synthase	2	-4.77	0.002
SPARC-like 1	4	-11.04	<0.001
Extracellular Superoxide Dismutase	4	-Inf.	<0.001

^a Paired student's t-test was used to determine the significant differences. Inf: infinity (denominator of 0: +Inf. not detected in uninfected, -Inf. not detected in SIVE).

($r = 0.87$) (Figure 1B), similar to that found in other shotgun proteomic as well as transcriptomic data.¹⁶

Following this validation, we analyzed the CSF of 4 animals at two time points: before SIV infection and when the animals were scheduled to be sacrificed due to neurological signs, shown to be due to SIV encephalitis (SIVE) at necropsy. One-hundred microliters CSF (from samples used in our previous metabolomic studies¹⁷) was extracted with methanol, and 10 μ g of the precipitated proteins used for proteomic analysis. LC-MS/MS and bioinformatics analysis revealed that a total of 113 different proteins were identified by at least 2 independent peptides and an MS/MS score >25 (Supplementary Table 1, Supporting Information). Since proteins with a normalized abundance of >0.2 had lower variation and more consistent detection in our validation experiments, we limited further analysis to the 73 proteins with an average abundance of >0.2 in either the uninfected or SIVE samples. A paired *t* test analysis revealed that 10 proteins were significantly ($p \leq 0.01$) changed (Table 2). Five of these were up-regulated in SIVE, and five down-regulated.

There are multiple possible mechanisms underlying differences in proteins in the CSF. A difference found in the CSF may reflect alterations in CSF production by the choroid plexus or absorption through the arachnoid villi, it may represent dysfunction of the blood-brain or blood-CSF barriers enabling plasma proteins to reach the CNS, or it may result from changes in CNS production of the proteins themselves. To examine the latter, we performed quantitative real-time polymerase chain reaction to examine the expression of the genes encoding the proteins identified as differing between the two conditions. RNA obtained from the hippocampus of the four animals studied by the proteomic analysis, as well as additional eight animals, was assessed for gene expression levels in comparison to that found in similar samples from nine control, uninfected monkeys. Indeed there was a significant increase in mRNA levels for all five of the up-regulated genes in the hippocampus of the SIVE monkeys (Figure 2). However, none of the five down-regulated proteins showed differences in gene expression between SIVE and control animals (data not shown).

IgM transcripts were the most highly increased (over 100-fold). To assess whether IgM gene expression changes indeed corresponded to protein expression in the brain, we examined brain tissue sections for the presence of IgM. Immunohistochemical analysis performed on SIVE brain sections showed

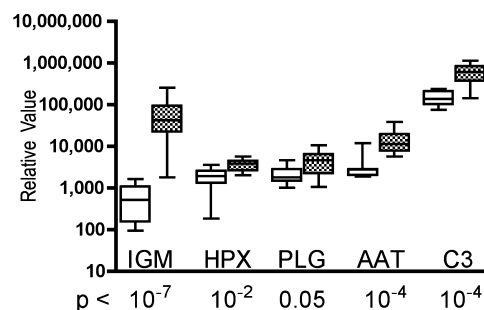


Figure 2. mRNA expression levels obtained by quantitative real time PCR using specific primers and probes as described in Table 1. Box and whisker plots (the box extends from the 25th to the 75th percentile, the line within the box is at the median, and the whiskers extend to the lowest and highest value) show the expression levels of the indicated genes in the hippocampus of control uninfected animals ($n = 9$, □) compared to that found in SIVE animals ($n = 12$, checkered boxes). The *p* values resulting from a Student's *t* test (on the \log_{10} transformed relative values) are indicated below each set of data. IGM, immunoglobulin M heavy chain; HPX, hemopexin; PLG, plasminogen; AAT, alpha-1-antitrypsin; C3, complement 3.

positive staining for IgM in cells (likely plasma cells) (Figure 3), which were not present in sections from uninfected animals (data not shown). Plasminogen transcripts were increased by much less than were those of IgM, slightly more than 2-fold. Immunohistochemical studies of brain tissue sections revealed that little to no plasminogen reactivity was present in the parenchyma of uninfected brains (Figure 4A, B) whereas in brains with SIVE positive staining was seen (Figure 4C, D, and E). In the choroid plexus, a mild level of staining was found in the epithelial cells in uninfected brains (Figure 4F) whereas in SIVE large strongly immunoreactive cells, likely macrophages, could also be found (Figure 4G).

Discussion

The ability of proteomics to yield fruitful biomarkers for disease has yet to reach its potential. This is especially true for neurodegenerative disorders, where the study of the most proximal biofluid, CSF, presents numerous difficulties. While a number of studies have utilized increased amounts of CSF, in combination with multistep paradigms to enable sensitive analysis, we investigated whether a simplified technique on relatively small amounts of CSF would be useful. Indeed, we found that methanol precipitation of 100 μ L of CSF yielded sufficient protein to identify proteins using LC-MS/MS, and that LC-MS/MS was a reproducible technique with this amount of protein. Using a primate model for HIV-induced neurodegenerative disease, we found proteins that were both increased and decreased in the presence of disease.

An increase in protein level in the CSF may come from several sources, including leakage from the plasma through a disruption in the blood-brain or blood-CSF barrier, increased production of these proteins in the choroid plexus and secretion into the CSF, and production in the brain parenchyma and drainage into the CSF. Since the up-regulated proteins are all normally present in the plasma at higher concentrations than the CSF, leakage of the normal CNS barriers represented a likely explanation, especially since we have reported increased amounts of albumin in the CSF of these animals during SIVE.¹⁷ However, examination of the expression of the genes encoding the up-regulated proteins revealed that all were significantly

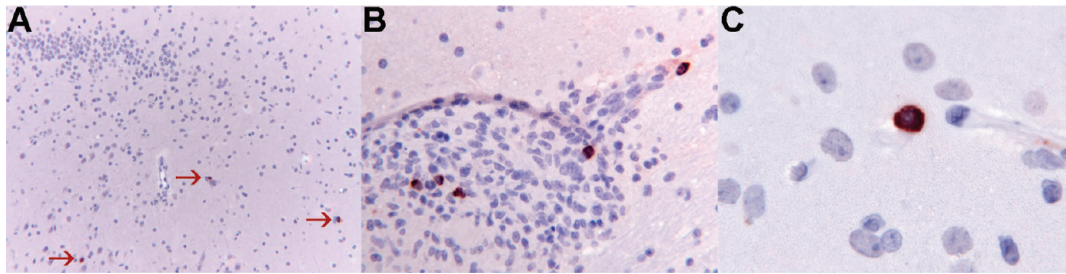


Figure 3. Photomicrographs of immunohistochemical analysis for IgM in the hippocampus of animals with SIVE. (A) Single immunoreactive cells (indicated by arrows) in an otherwise pathologically unremarkable region (original magnification 200 \times). (B) Immunoreactive cells within an inflammatory infiltrate (original magnification 500 \times). (C) High power micrograph of an individual immunoreactive cell (original magnification 1250 \times).

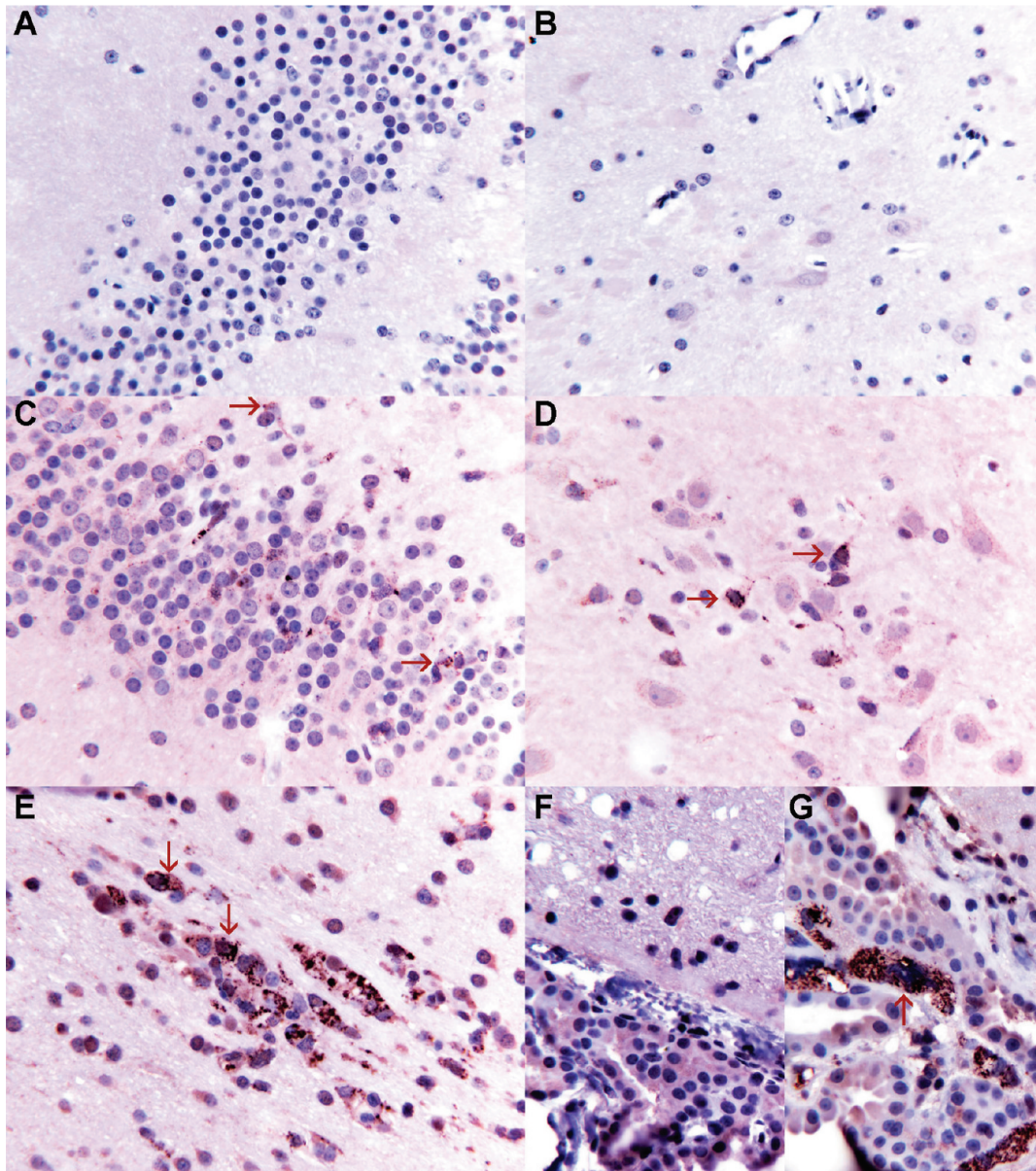


Figure 4. Photomicrographs of immunohistochemical analysis for plasminogen in the brains of uninfected animals and those with SIVE. Original magnification of 500 \times for all. (A, B) Brain sections from uninfected animals. (C, D, and E). Sections from animals with SIVE, examples of positive cells shown with arrows. (F, G) Choroid plexus from uninfected (F) and SIVE (G), example of positive cell in latter shown with arrow.

increased in the brains of affected animals, indicating that brain production likely plays a substantial role in their presence in the CSF during disease. This raises a caution for methods

utilizing immunodepletion products based on removing plasma proteins, as many of these are indeed produced within the CNS and can play neuropathogenic roles. While IgM positive cells

were predominantly located in the brain parenchyma, we found that plasminogen positive cells were located in the parenchyma as well as the choroid plexus. The latter may help explain the difference found in plasminogen protein up-regulation in the CSF by our proteomic technique (12-fold) and the difference found in brain parenchymal plasminogen mRNA by real-time PCR (2.3-fold).

There are some clues regarding the potential role of these up-regulated proteins in CNS pathology. IgM is the first immunoglobulin made when humoral immunity is stimulated, and it has been suggested that intrathecal IgM synthesis is an onset marker in the autoimmune CNS disorder multiple sclerosis.¹⁸ However its function in the brain in SIV or HIV infection is not clear, and it would be of interest to assess whether such antibodies are directed against the virus itself, or other specificities. Autoimmune antibody antibodies have also been found in individuals with HIV dementia, but their role in the disease process is unknown.¹⁹ Complement component C3 is also a major immune product, and its presence and production by astrocytes, microglia and to a lesser extent neurons has been documented in SIVE²⁰ as well as human CNS disorders including Alzheimer's disease (AD) and multiple sclerosis.²¹

The enhanced complement synthesis may possibly enable a fast and effective immune activation after infection, leading to the formation of molecules such as the anaphylatoxins C3a and C5a, which act as chemoattractants and activators of macrophages and microglia, and may act through these cells or other mechanisms to protect the brain.^{22–24} However, chronic activation of the complement has been associated with pathogenesis in AD and multiple sclerosis.^{25–28} Furthermore, during CNS development, C3 is associated with synaptic elimination.²⁹ Thus in this case increased C3 likely contributes to SIV induced damage to the brain.

Increases in two of the other up-regulated proteins have been found in certain CNS disorders. Hemopexin, which functions in scavenging the heme released or lost by the turnover of heme proteins like hemoglobin, has been shown to be up-regulated in the CSF of AD patients.³⁰ Alpha-1-antitrypsin, a glycoprotein belonging to the family of serine proteases, has also been shown to be up-regulated in the CSF of AD,³¹ as well as traumatic brain injury³² and more recently in Guillain-Barre syndrome patients.³³

The final protein, plasminogen is a precursor enzyme which following partial cleavage by its activators is converted to its active and proteolytic form, plasmin. Whether such activation occurs here is not known. While not studied in neurodegenerative disorders, plasminogen can be induced in the brain by treatment with the excitatory glutamate analogue kainite.³⁴

Although we could find evidence of increased gene expression for the up-regulated proteins in the brain, we could not find differences in the expression of the genes encoding the down-regulated ones. There are multiple reasons that this might be the case. One possibility is that the differences in protein levels do not correspond to changes in RNA levels. In addition to various post-transcriptional regulatory mechanisms, other processes leading to increased protein degradation or clearance from the CSF could lead to these results. Furthermore, these proteins may be made in the choroid plexus and secreted into the CSF, and we did not examine change in the regulation of choroid plexus gene expression. Additionally, the decrease itself may result from the experimental design due to a relative differential loading. For example if certain proteins,

such as extracellular superoxide dismutase (Table 2), are at the limit of detection in normal CSF, in the diseased state they can become diluted by the increase of other proteins to drive them to undetectable concentrations, giving an "infinite" decrease ratio between normal and diseased which may not be statistically or biologically relevant.

Disadvantages that tend to pose daunting tasks in CSF profiling include its limited availability and large dynamic range of proteins that can extend several orders of magnitude between the highest and lowest expressed proteins. While little can be done about the former, several strategies, including immunodepletion of abundant proteins followed by multidimensional separations have been employed in identifying novel biomarkers for neurodegenerative diseases. In fact a recent study employed such immunodepletion followed by 2D-DIGE and then mass spectrometry to identify changes in the CSF proteomes that differentiated HAD from HIV infected individuals without CNS disease.³⁵ Due to the amount of protein needed and limited amount of sample, only six of the 38 samples (16%) could be assessed by this method. Still, this study was successful in identifying six putative biomarkers: vitamin D binding protein, clusterin, gelsolin, complement C3, procollagen C-endopeptidase enhancer 1, and cystatin C. Five of these proteins were indeed detected by our technique (Table 2), and one of them, C3, was also found to be differentially regulated in our study. However, whereas the 2D-DIGE study of Rozek et al.³⁵ found C3 was down-regulated, we find that C3 is up-regulated. The numerous differences, including humans vs monkeys, lumbar vs cisterna magna CSF, cross-sectional study vs before-after in the same subjects, selection of samples based on protein content vs use of all samples, immunodepletion vs methanol precipitation, and 2D-DIGE followed by MS/MS vs LC-MS/MS, make determination of the reasons for the differences difficult.

In addition to these methods, surface enhanced laser desorption ionization (SELDI) has been utilized to identify biomarkers in the CSF for HIV CNS disease.^{36,37} However the use of the SELDI platform for biomarker discovery has been problematic.^{38,39} Still, a recent study used SELDI to identify increases in Chitinase 3-like 1 (also known as HCgp39 and YKL-40) in the CSF as a biomarker of SIVE.⁴⁰ In our previous microarray studies of SIVE we had indeed found increased gene transcription and brain parenchymal localization of expression of Chitinase 3-like 1.⁴¹ In our current proteomics study this protein was elevated (by 2.7-fold) in SIVE, however the difference between the groups did not reach statistical significance. We had also identified an increase in gene transcription osteopontin in SIVE brains,¹⁷ and follow-up enzyme-linked immunosorbant assay (ELISA) revealed its increase in the CSF.^{42,43} Yet in our current study the relatively low level of detection of osteopontin precluded its assessment. No single technique is ideal in the search for biomarkers, and complementary information can be obtained from unbiased profiling, whether by 2D-DIGE, SELDI, multidimensional protein identification technology, our technique or others, as well as from directed studies such as ELISA, multianalyte profiling, and immunohistochemistry. As with our study combining metabolomics with gene array profiling,¹⁷ the combination of gene expression analysis and/or metabolomics with proteomics can be a great asset in the search for valid biomarkers.

The dramatically increased power of new analytical technologies together with bioinformatics approaches promises to provide a more comprehensive picture of proteins and changes

in the CSF. The ability to obtain relative quantification of proteins by MS using techniques such as isotope tagged absolute and relative quantitation (iTRAQ), which allows the comparison of multiple different specimens at once, is promising. CSF proteomics using iTRAQ has been used to identify proteins that differentiated AD, Parkinson's disease and dementia with Lewy bodies patients from each other as well as the controls.⁴⁴ Future increased sensitivity of MS analysis would aid approaches such as that described here. In addition, if available, larger volumes of CSF could be useful, perhaps combined with additional pre-MS separation techniques, enabling the identification of more proteins. However additional steps can greatly increase variability, and we believe one key to our ability to identify and verify the up-regulated proteins is the precision of our technique, and the reproducibility of any additional methodologies would need verification. We also note that we chose the methanol precipitation based on its utility for removing proteins from solution to enable metabolomic analysis. A comparison of different methods for protein isolation may further optimize this method of CSF proteomic analysis.

In addition to CSF analysis in neurodegenerative and neuroinfectious diseases, this technique can be readily applied to other biomedical conditions. For example it can be utilized for biofluids, which similar to CSF, are difficult to obtain in large quantities, such as interstitial fluid in a region of tissue pathology, cyst contents, breast or other ductal fluid, and tears. The same also applies for other biofluids like synovial fluid from joints and bronchioalveolar lavage from lungs that can serve as ideal sources for identifying biomarkers for arthritis and pulmonary diseases, respectively.

Conclusions

Our study highlights a relatively simple proteomic characterization of CSF proteins that allows semiquantitative comparisons. This technique was used to identify fingerprints for SIV associated neuropathology, modeling the dementia that can result from HIV infection. These resulting biomarkers then revealed an important facet of the disease—that their presence does not just reflect the breakdown of the normal barriers that isolate the CNS, but that the expression of the genes encoding these proteins are markedly increased in the brain parenchyma itself during disease.

Abbreviations: ACN, acetonitrile; AD, Alzheimers disease; CNS, central nervous system; CSF, cerebrospinal fluid; ELISA, enzyme-linked immunosorbant assay; HAART, highly active antiretroviral therapy; HAND, HIV-associated neurological disorders; HIV, human immunodeficiency virus; iTRAQ, isotope tagged absolute and relative quantitation; LC, liquid chromatography; MS, mass spectrometry; SELDI, surface enhanced laser desorption ionization; SIV, simian immunodeficiency virus; SIVE, SIV encephalitis; SPI, scored peak intensity.

Acknowledgment. We thank Claudia Flynn and Michelle Zandonatti for assistance with the real-time PCR, and Carly Ninemire and Dr. Jun Tian for assistance with the immunohistochemistry. This is manuscript # 19641 from TSRI and # 2 from the UNMC CITN. This work was supported by NIH grants MH073490, MH062261, and DA026146 awarded to H.S.F., and MH062512 to Dr. Igor Grant, UCSD.

Supporting Information Available: Supplemental Table 1. This material is available free of charge via the Internet at <http://pubs.acs.org>.

References

- (1) McArthur, J. C.; Brew, B. J.; Nath, A. Neurological complications of HIV infection. *Lancet Neurol.* **2005**, *4* (9), 543–55.
- (2) Brew, B. J. Evidence for a change in AIDS dementia complex in the era of highly active antiretroviral therapy and the possibility of new forms of AIDS dementia complex. *AIDS* **2004**, *18* (1), S75–8.
- (3) Coon, K. D.; Dunckley, T.; Stephan, D. A. Biomarker identification in neurologic diseases: improving diagnostics and therapeutics. *Expert Rev. Mol. Diagn.* **2004**, *4* (3), 361–75.
- (4) Rifai, N.; Gillette, M. A.; Carr, S. A. Protein biomarker discovery and validation: the long and uncertain path to clinical utility. *Nat. Biotechnol.* **2006**, *24* (8), 971–83.
- (5) Milhorat, T. H. Choroid plexus and cerebrospinal fluid production. *Science* **1969**, *166* (3912), 1514–6.
- (6) Milhorat, T. H.; Hammock, M. K.; Fenstermacher, J. D.; Levin, V. A. Cerebrospinal fluid production by the choroid plexus and brain. *Science* **1971**, *173* (994), 330–2.
- (7) Thompson, E. J. Cerebrospinal fluid. *J. Neurol. Neurosurg. Psychiatry* **1995**, *59* (4), 349–57.
- (8) Kanekiyo, T.; Ban, T.; Aritake, K.; Huang, Z. L.; Qu, W. M.; Okazaki, I.; Mohri, I.; Murayama, S.; Ozono, K.; Taniike, M.; Goto, Y.; Urade, Y. Lipocalin-type prostaglandin D synthase/beta-trace is a major amyloid beta-chaperone in human cerebrospinal fluid. *Proc. Natl. Acad. Sci. U.S.A.* **2007**, *104* (15), 6412–7.
- (9) Thouvenot, E.; Urbach, S.; Dantec, C.; Poncet, J.; Seveno, M.; Demetree, E.; Jouin, P.; Touchon, J.; Bockaert, J.; Marin, P. Enhanced Detection of CNS Cell Secretome in Plasma Protein-Depleted Cerebrospinal Fluid. *J. Proteome Res.* **2008**, *7* (10), 4409–4421.
- (10) Pan, S.; Zhu, D.; Quinn, J. F.; Peskind, E. R.; Montine, T. J.; Lin, B.; Goodlett, D. R.; Taylor, G.; Eng, J.; Zhang, J. A combined dataset of human cerebrospinal fluid proteins identified by multi-dimensional chromatography and tandem mass spectrometry. *Proteomics* **2007**, *7* (3), 469–73.
- (11) Fox, H. S.; Gold, L. H.; Henriksen, S. J.; Bloom, F. E. Simian immunodeficiency virus: a model for neuroAIDS. *Neurobiol. Dis.* **1997**, *4* (3–4), 265–74.
- (12) Fox, H. S. Primate Models for NeuroInfectious Diseases: Lessons from SIV. *J. Neurovirol.* **2008**, in press.
- (13) Liu, H.; Sadygov, R. G.; Yates, J. R. 3rd, A model for random sampling and estimation of relative protein abundance in shotgun proteomics. *Anal. Chem.* **2004**, *76* (14), 4193–201.
- (14) Shen, Z.; Want, E. J.; Chen, W.; Keating, W.; Nussbaumer, W.; Moore, R.; Gentle, T. M.; Siuzdak, G. Sepsis plasma protein profiling with immunodepletion, three-dimensional liquid chromatography tandem mass spectrometry, and spectrum counting. *J. Proteome Res.* **2006**, *5* (11), 3154–60.
- (15) Zhang, B.; VerBerkmoes, N. C.; Langston, M. A.; Uberbacher, E.; Hettich, R. L.; Samatova, N. F. Detecting differential and correlated protein expression in label-free shotgun proteomics. *J. Proteome Res.* **2006**, *5* (11), 2909–18.
- (16) Pavelka, N.; Fournier, M. L.; Swanson, S. K.; Pelizzola, M.; Ricciardi-Castagnoli, P.; Florens, L.; Washburn, M. P. Statistical similarities between transcriptomics and quantitative shotgun proteomics data. *Mol. Cell. Proteomics* **2008**, *7* (4), 631–44.
- (17) Wikoff, W. R.; Pendyala, G.; Siuzdak, G.; Fox, H. S. Metabolomic analysis of the cerebrospinal fluid reveals changes in phospholipase expression in the CNS of SIV-infected macaques. *J. Clin. Invest.* **2008**, *118* (7), 2661–9.
- (18) Villar, L. M.; Masjuan, J.; Gonzalez-Porcu, P.; Plaza, J.; Sadaba, M. C.; Roldan, E.; Bootello, A.; Alvarez-Cermeno, J. C. Intrathecal IgM synthesis predicts the onset of new relapses and a worse disease course in MS. *Neurology* **2002**, *59* (4), 555–9.
- (19) Schutzer, S. E.; Brunner, M.; Fillit, H. M.; Berger, J. R. Autoimmune markers in HIV-associated dementia. *J. Neuroimmunol.* **2003**, *138* (1–2), 156–61.
- (20) Speth, C.; Williams, K.; Hagleitner, M.; Westmoreland, S.; Rambach, G.; Mohsenipour, I.; Schmitz, J.; Wurzner, R.; Lass-Flörl, C.; Stoiber, H.; Dierich, M. P.; Maier, H. Complement synthesis and activation in the brain of SIV-infected monkeys. *J. Neuroimmunol.* **2004**, *151* (1–2), 45–54.
- (21) Morgan, B. P.; Gasque, P.; Singhrao, S.; Piddlesden, S. J. The role of complement in disorders of the nervous system. *Immunopharmacology* **1997**, *38* (1–2), 43–50.

- (22) Nolte, C.; Moller, T.; Walter, T.; Kettenmann, H. Complement 5a controls motility of murine microglial cells in vitro via activation of an inhibitory G-protein and the rearrangement of the Actin cytoskeleton. *Neuroscience* **1996**, *73* (4), 1091–107.
- (23) Osaka, H.; Mukherjee, P.; Aisen, P. S.; Pasinetti, G. M. Complement-derived anaphylatoxin C5a protects against glutamate-mediated neurotoxicity. *J. Cell Biochem.* **1999**, *73* (3), 303–11.
- (24) Boos, L.; Szalai, A. J.; Barnum, S. R. C3a expressed in the central nervous system protects against LPS-induced shock. *Neurosci. Lett.* **2005**, *387* (2), 68–71.
- (25) Eikelenboom, P.; Hack, C. E.; Rozemuller, J. M.; Stam, F. C. Complement activation in amyloid plaques in Alzheimer's dementia. *Virchows Arch. B: Cell Pathol. Incl. Mol. Pathol.* **1989**, *56* (4), 259–62.
- (26) Veerhuis, R.; Janssen, I.; Hack, C. E.; Eikelenboom, P. Early complement components in Alzheimer's disease brains. *Acta Neuropathol.* **1996**, *91* (1), 53–60.
- (27) Yasojima, K.; Schwab, C.; McGeer, E. G.; McGeer, P. L. Up-regulated production and activation of the complement system in Alzheimer's disease brain. *Am. J. Pathol.* **1999**, *154* (3), 927–36.
- (28) Gasque, P.; Neal, J. W.; Singhrao, S. K.; McGreal, E. P.; Dean, Y. D.; Van, B. J.; Morgan, B. P. Roles of the complement system in human neurodegenerative disorders: pro-inflammatory and tissue remodeling activities. *Mol. Neurobiol.* **2002**, *25* (1), 1–17.
- (29) Stevens, B.; Allen, N. J.; Vazquez, L. E.; Howell, G. R.; Christopherson, K. S.; Nouri, N.; Micheva, K. D.; Mehalow, A. K.; Huberman, A. D.; Stafford, B.; Sher, A.; Litke, A. M.; Lambris, J. D.; Smith, S. J.; John, S. W.; Barres, B. A. The classical complement cascade mediates CNS synapse elimination. *Cell* **2007**, *131* (6), 1164–78.
- (30) Castano, E. M.; Roher, A. E.; Esh, C. L.; Kokjohn, T. A.; Beach, T. Comparative proteomics of cerebrospinal fluid in neuropathologically-confirmed Alzheimer's disease and non-demented elderly subjects. *Neurol. Res.* **2006**, *28* (2), 155–63.
- (31) Nielsen, H. M.; Minthon, L.; Londos, E.; Blennow, K.; Miranda, E.; Perez, J.; Crowther, D. C.; Lomas, D. A.; Janciauskiene, S. M. Plasma and CSF serpins in Alzheimer disease and dementia with Lewy bodies. *Neurology* **2007**, *69* (16), 1569–79.
- (32) Conti, A.; Sanchez-Ruiz, Y.; Bachi, A.; Beretta, L.; Grandi, E.; Beltramo, M.; Alessio, M. Proteome study of human cerebrospinal fluid following traumatic brain injury indicates fibrin(ogen) degradation products as trauma-associated markers. *J. Neurotrauma* **2004**, *21* (7), 854–63.
- (33) Yang, Y. R.; Liu, S. L.; Qin, Z. Y.; Liu, F. J.; Qin, Y. J.; Bai, S. M.; Chen, Z. Y. Comparative Proteomics Analysis of Cerebrospinal Fluid of Patients with Guillain-Barre Syndrome *Cell. Mol. Neurobiol.* **2008**, *28* (5), 737–44.
- (34) Sharon, R.; Abramovitz, R.; Miskin, R. Plasminogen mRNA induction in the mouse brain after kainate excitation: codistribution with plasminogen activator inhibitor-2 (PAI-2) mRNA. *Brain Res. Mol. Brain Res.* **2002**, *104* (2), 170–5.
- (35) Rozek, W.; Ricardo-Dukelow, M.; Holloway, S.; Gendelman, H. E.; Wojna, V.; Melendez, L. M.; Ciborowski, P. Cerebrospinal fluid proteomic profiling of HIV-1-infected patients with cognitive impairment. *J. Proteome Res.* **2007**, *6* (11), 4189–99.
- (36) Berger, J. R.; Avison, M.; Mootoor, Y.; Beach, C. Cerebrospinal fluid proteomics and human immunodeficiency virus dementia: preliminary observations. *J. Neurovirol.* **2005**, *11* (6), 557–62.
- (37) Laspiur, J. P.; Anderson, E. R.; Ciborowski, P.; Wojna, V.; Rozek, W.; Duan, F.; Mayo, R.; Rodriguez, E.; Plaud-Valentin, M.; Rodriguez-Orengo, J.; Gendelman, H. E.; Melendez, L. M. CSF proteomic fingerprints for HIV-associated cognitive impairment. *J. Neuroimmunol.* **2007**, *192* (1–2), 157–70.
- (38) Baggerly, K. A.; Morris, J. S.; Coombes, K. R. Reproducibility of SELDI-TOF protein patterns in serum: comparing datasets from different experiments. *Bioinformatics* **2004**, *20* (5), 777–85.
- (39) Liotta, L. A.; Petricoin, E. F. Putting the "bio" back into biomarkers: orienting proteomic discovery toward biology and away from the measurement platform. *Clin. Chem.* **2008**, *54* (1), 3–5.
- (40) Bonneh-Barkay, D.; Bissel, S. J.; Wang, G.; Fish, K. N.; Nicholl, G. C.; Darko, S. W.; Medina-Flores, R.; Murphey-Corb, M.; Rajakumar, P. A.; Nyaundi, J.; Mellors, J. W.; Bowser, R.; Wiley, C. A. YKL-40, a marker of simian immunodeficiency virus encephalitis, modulates the biological activity of basic fibroblast growth factor. *Am. J. Pathol.* **2008**, *173* (1), 130–43.
- (41) Roberts, E. S.; Zandonatti, M. A.; Watry, D. D.; Madden, L. J.; Henriksen, S. J.; Taffe, M. A.; Fox, H. S. Induction of Pathogenic Sets of Genes in Macrophages and Neurons in NeuroAIDS. *Am. J. Pathol.* **2003**, *162* (6), 2041–57.
- (42) Burdo, T. H.; Ellis, R. J.; Fox, H. S. Osteopontin is increased in HIV-associated dementia. *J. Infect. Dis.* **2008**, *198* (5), 715–22.
- (43) Burdo, T. H.; Wood, M. R.; Fox, H. S. Osteopontin prevents monocyte recirculation and apoptosis. *J. Leukoc. Biol.* **2007**, *81* (6), 1504–11.
- (44) Abdi, F.; Quinn, J. F.; Jankovic, J.; McIntosh, M.; Leverenz, J. B.; Peskind, E.; Nixon, R.; Nutt, J.; Chung, K.; Zabetian, C.; Samii, A.; Lin, M.; Hattar, S.; Pan, C.; Wang, Y.; Jin, J.; Zhu, D.; Li, G. J.; Liu, Y.; Waichunas, D.; Montine, T. J.; Zhang, J. Detection of biomarkers with a multiplex quantitative proteomic platform in cerebrospinal fluid of patients with neurodegenerative disorders. *J. Alzheimers Dis.* **2006**, *9* (3), 293–348.

PR800854T